

Potential of optical microangiography to monitor cerebral blood perfusion and vascular plasticity following traumatic brain injury in mice *in vivo*

Yali Jia,^a Nabil Alkayed,^b and Ruikang K. Wang^{a,b,*}

^aOregon Health and Science University, Department of Biomedical Engineering, 3303 South West Bond Avenue, Portland, Oregon 97239

^bOregon Health and Science University, Department of Anesthesiology and Peri-Operative Medicine, 3181 South West Sam Jackson Park Road, Portland, Oregon 97239

Abstract. Optical microangiography (OMAG) is a recently developed imaging modality capable of volumetric imaging of dynamic blood perfusion, down to capillary level resolution, with an imaging depth up to 2.00 mm beneath the tissue surface. We report the use of OMAG to monitor the cerebral blood flow (CBF) over the cortex of mouse brain upon traumatic brain injury (TBI), with the cranium left intact, for a period of two weeks on the same animal. We show the ability of OMAG to repeatedly image 3-D cerebral vasculatures during pre- and post-traumatic phases, and to visualize the changes of regulated CBF and the vascular plasticity after TBI. The results indicate the potential of OMAG to explore the mechanism involved in the rehabilitation of TBI. © 2009 Society of Photo-Optical Instrumentation Engineers. [DOI: 10.1117/1.3207121]

Keywords: Optical microangiography; cerebral blood perfusion; vascular remodeling; traumatic brain injury.

Paper 09162L received Apr. 23, 2009; accepted for publication Jun. 29, 2009; published online Aug. 25, 2009.

Traumatic brain injury (TBI) often causes alterations in cerebral blood flow (CBF) that are thought to influence secondary pathophysiology and neurologic outcome in human brain. Inadequate CBF is an important contributor to mortality and morbidity after TBI.¹ Despite the importance of cerebral vascular dysfunction in TBI pathophysiology, the effect of trauma on CBF has been less well studied than the effect of trauma on the brain.² Similarly, our understanding of the rehabilitation and autoregulation of cerebrovascular blood circulation after TBI remains incomplete. In this regard, a non-invasive technique for imaging *in vivo* blood flow, down to capillary level resolution, would be of great value.

Although a number of imaging techniques have made contributions to our understanding of healing mechanisms of TBI by imaging the CBF and its volume changes over the cortex in animal models, important limitations still remain—such as

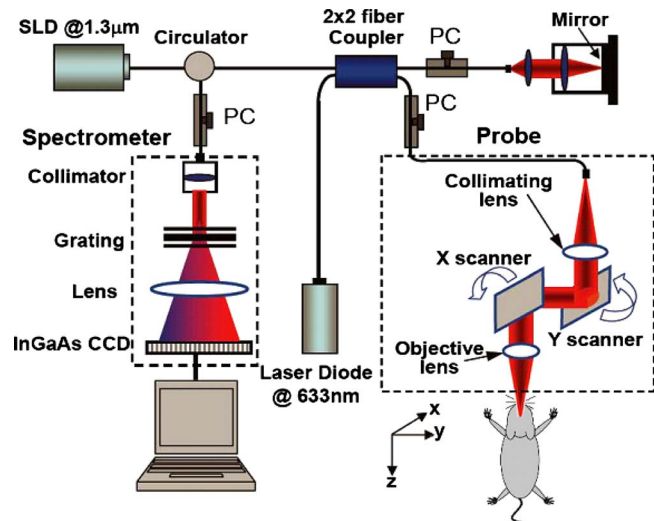


Fig. 1 Schematic of the OMAG system used to collect the 3-D spectral interferogram data cube to perform the 3-D angiography of traumatic brain tissue in the small animal model *in vivo*. CCD represents the charge coupled device, and PC the polarization controller.

invasiveness (e.g., radioactive approaches³), their incapability of providing 3-D information (e.g., laser speckle imaging⁴), their inability to provide adequate spatial and temporal resolutions (e.g., MRI⁵), and their inability to image beyond shallow (>300 μm) depths (e.g., confocal⁶). What is often needed is a real-time imaging technique that is capable of visualizing vessels and blood flow in 3-D at a high resolution (e.g., <10 μm), so that the detailed functional architecture of the perfused microvascular network can be revealed.

Optical microangiography (OMAG)⁷ is a recently developed imaging modality that is capable of imaging dynamic blood flow, down to capillary level resolution, within tissue beds up to 2.00 mm beneath the tissue surface. Imaging contrast of blood perfusion in OMAG is based on endogenous light scattering from moving blood cells; thus, no exogenous contrast agents are necessary for imaging. Imaging is achieved by the efficient separation of the moving scattering elements from the static scattering ones within an illuminated tissue. In essence, OMAG mathematically maps the backscattered optical signals from the moving particles into one image—that is, the blood flow image—while it simultaneously maps the backscattered optical signals from the static particles into a second image, which is the microstructural image. By use of the OMAG imaging technique, Wang and Hurst demonstrated *in vivo* imaging of cerebral vascular circulation of adult living mice, down to capillary level, with the skull and skin left intact.⁸ In an attempt to show the potential of OMAG to visualize the dysfunctional microcirculation after TBI, we used OMAG to noninvasively monitor the changes of CBF over days on the same experimental animal.

Figure 1 illustrates the OMAG system used in this study that is similar to the one described previously.⁸ Briefly, the system employed a broadband infrared superluminescent diode (Denselight, Singapore) with a central wavelength of 1300 nm to illuminate the tissue. The light emerging at the output of interferometer was sent to a home-built high-speed

*Address all correspondence to: Ruikang K. Wang, E-mail: r.k.wang@bme.ogi.edu

spectrometer that employed a line scan infrared InGaAs detector to capture the backscattering light emerged from the illuminated tissue surface. The system has the imaging resolution of $16 \times 16 \times 8 \mu\text{m}^3$ at the x - y - z imaging direction, and an imaging depth of ~ 3 mm in air. The imaging rate was 17,000 axial scans (A scan) per second in this study. The 3-D imaging of tissue sample *in vivo* was performed by an x - y galvanometer scanner with a scanning priority in the x direction (B scan). The x scanner was driven by a 16-Hz sawtooth waveform to provide a B scan over ~ 2.5 mm at the sample, while the y scanner was driven by a ~ 0.03 -Hz sawtooth waveform that provided the beam scanning in the elevational direction also of ~ 2.5 mm. The minimal flow velocity that can be detected by the system was $\sim 260 \mu\text{m/s}$.

Three-month-old C57 BL/6 mice (20 to 30 g) were used in the study to show the potential of OMAG monitoring of changes of dynamic CBF following TBI *in vivo*. The experimental protocol was in compliance with the Federal guidelines for care and handling of small rodents and approved by the Institutional Animal Care and Use Committee. Prior to OMAG imaging, the mouse head was shaved and depilated. During imaging, the animal was immobilized in a custom-made stereotaxic stage and was lightly anesthetized with isoflurane (0.2-L/min O_2 , 0.8-L/min air). The body temperature was kept between 35.5 to 36.5 °C, and monitored by a rectal thermal probe throughout the experiment. An incision of ~ 1 cm was made along the sagittal suture, and the frontal parietal and interparietal bones were exposed by pulling the skin to the sides. The animal was then positioned under the OMAG scanning probe. To acquire the CBF images over a large area of the cortex, the scan was performed clockwise, which resulted in six OMAG images covering areas between the anterior coronal suture (Bregma) and posterior coronal suture (Lambda). The total imaging acquisition time for six OMAG scans was ~ 8 min. For each 3-D OMAG image, a volumetric segmentation algorithm⁸ was applied to isolate the blood flow signals within the cortex, and a maximum projection method was then used to project the blood flow signals into the x - y plane to reduce the image size. The final image, representing the CBF over the mouse cortex, was obtained by stitching six resulted images together and cropping, covering an area of $\sim 4.2 \times 7.2 \text{ mm}^2$ over the mouse head.

Before inducing TBI, a control OMAG image was acquired as the baseline for later comparisons. Then the mouse was subjected to TBI. To induce a traumatic lesion in the cortex, a 30-gauge needle was disinfected and used to puncture a round and vertical hole with a depth of 1.5 mm measured from the surface of skull. The bleeding was washed out using medical grade saline. After 30 min onset of TBI, OMAG imaging was initiated at the same region as the control. After imaging, the animal was sutured, disinfected, and injected with antibiotics, and then returned to the cage for rehabilitation. A series of OMAG imaging was taken on the same animal at day 1 (24 h after TBI), 4, 7, and 10, respectively. At last, the animal was euthanized by cervical dislocation and digital images were taken (Roper Scientific Photometrics Coolsnap cf) of the head. Next, the skin and skull on the head were carefully removed to expose the dorsal blood vessels of the brain, which were then photographed for comparison with those obtained *in vivo* from the OMAG system.

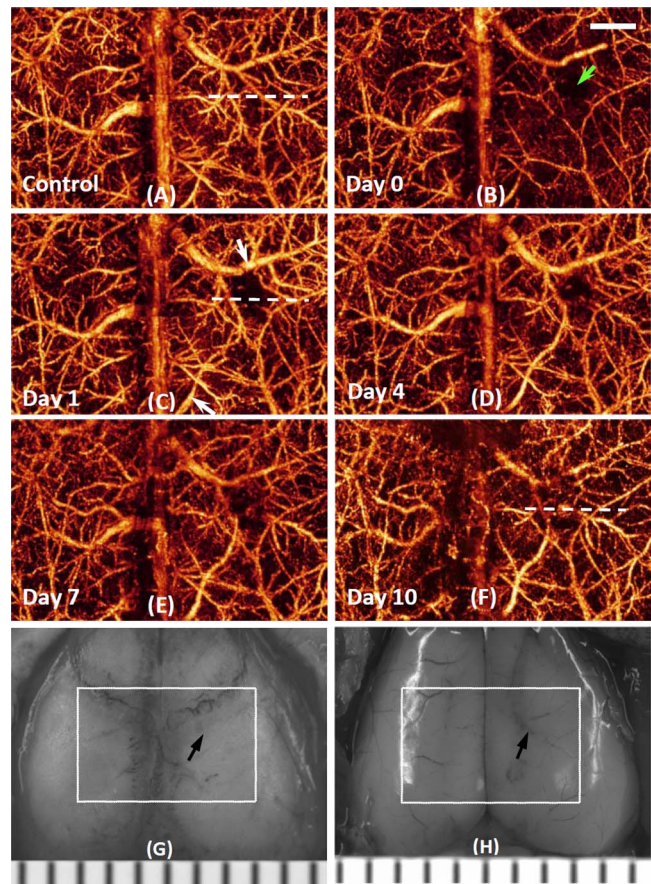


Fig. 2 Serial 3-D OMAG imaging of the cortex during TBI in mice *in vivo* at different time points as shown. Compared to baseline (a), progressive vessel regulation (vessels pointed by white arrows) and neovascularization at traumatic areas develop during TBI rehabilitation. The site of injury is pointed by the green arrow. (g) and (h) are the photographs of the brain cortex with and without skull on the same mouse. The image size in (a) through (f) is $\sim 7.2 \times 4.2 \text{ mm}^2$, corresponding to the area marked with a dashed white box in (g) and (h). The scale bar=1.0 mm. (Color online only.)

A typical series of OMAG CBF images is shown in Fig. 2, and the cross sectional structural and blood perfusion images corresponding to the positions marked by the dash lines in Fig. 2(a) are shown in Fig. 3. Figure 2(a) is the OMAG image from baseline where it shows the capability of OMAG to delineate the dynamic CBF, down to capillary level resolution, within the cortex while the skull was left intact. At 30 min after TBI, a reduction of CBF (cerebral ischemia) over the entire cortex was seen in the OMAG image [Fig. 2(b)]. The reduction of CBF might be due to the post-traumatic hemorrhage caused by the external injury that leaves the blood in the space between the meninges and cortex, near the TBI site (pointed by the green arrow). However, the CBF reduction was not even across the cortex, as seen in Fig. 2(b), with the ipsilateral reduction more severe than the contralateral region. Another possible reason for the reduction of CBF seen in the OMAG image might be the possible bleeding that partially blocks the light penetration into the deeper tissues (i.e., light absorption due to the clotted blood): however, the clotted blood will be most likely localized near the TBI site. At the TBI site, blood flow was totally ceased

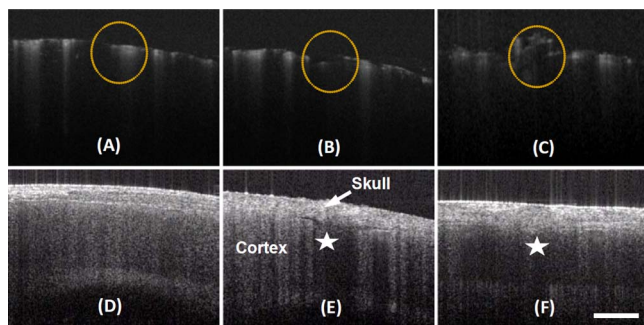


Fig. 3 Cross sectional images (slices) of blood flow (top row) and corresponding microstructures (bottom row) of the mouse brain during [(a) and (d)] pre- and [(b) and (e), (c) and (f)] post-traumatic phases. They correspond to the dashed lines marked in Fig. 2. The areas in the brown dashed circle show the evolution of neovascularization and the trauma zone in the cortex is identified by a white star.

due to hemostasis. Furthermore, the vessel constriction (decrease of the diameter of blood vessels) was apparent in the ipsilateral region that might be caused by acute cerebrovascular regulation to prevent the occurrence of hypoxic-ischemic reaction.⁹

During the progress of rehabilitation, OMAG is able to visualize the changes of CBF on the same injured animal over time. At day 1, vasoconstriction disappeared and the blood perfusion almost returned to the baseline, apart from the site at injury [Fig. 2(c)]. However, the vessel dilation seemed to occur near the TBI site, particularly for the vessels pointed by the white arrows and their associated branches. The needle-induced lesion area is still absent from the blood circulation [Figs. 2(c) and 3(b)]. From day 4 to day 7, the new blood vessels started to appear in the traumatic region, indicating the neovascularization was happening [Figs. 2(d) and 2(e)]. The neovascularization was more evident at day 10 [Figs. 2(f) and 2(c)]; however, the blood flow over the cortex seen in previous OMAG images was increasingly difficult to detect by the OMAG system at day 10. The reason for this difficulty is because the thickness of the cranium doubled [Fig. 3(f)] when compared with the control [Fig. 3(d)] that reduced the amount of light to reach the cortex because of the well-known light scattering phenomenon. The increased thickness of cranium was most probably due to the infection caused by the experimental procedures, although the antibiotics were applied daily to the animal. This can be eliminated for future systematic studies on TBI through careful and skilled surgical procedures. Despite this infection in the current study that doubled the cranium thickness, OMAG still offers the opportunity to visualize the changes of global CBF that may aid our understanding of the cerebral vascular plasticity upon TBI.

For comparison, the direct photographs of the brain cortex with and without skull just after the OMAG imaging at day 10 are shown in Figs. 2(g) and 2(h), respectively, where the TBI site is identified by the black arrow. Seeing the blood vessels through the cranium is almost impossible [Fig. 2(g)]. Comparing Fig. 2(h) and the OMAG images, agreement on the major vascular network over the brain cortex is achieved. More important, the microvessels unobserved in the photograph of Fig. 2(h) are seen in OMAG images, suggesting OMAG's capability to monitor the cerebral vascular circulation after TBI at capillary level resolution.

The ability to noninvasively map the variations of cerebral blood flow would greatly contribute to our understanding of the complex nature involved following TBI. Because the moving red blood cells in patent vessels, including capillaries, can be precisely localized in OMAG, any functional vessel up to a depth of 2.00 mm is able to be imaged under OMAG. Our current experimental results have shown the capability of OMAG to monitor the response of the cerebral circulation to TBI, and to visualize neovascularization following TBI. The noted increases in newly formed vessels after TBI may serve to alleviate secondary neuronal damage by improving local blood flow and metabolite delivery to the nutrient-deprived neurons. Our understanding of the mechanism of new vessel formation still remains incomplete. Based on the volumetric imaging of OMAG with improved resolution, OMAG may provide a powerful tool to investigate neovascularization following TBI on the same animal over a long period of time. Specifically, if combined with immunocytochemistry, OMAG may aid the investigation of elucidating whether both angiogenesis and vasculogenesis or either of them participates in promoting neovascularization.¹⁰ However, due to the coagulation of red blood cells from broken vessels on the site of injury in the current study, observation of the generation of precursor microvessels will possibly be inhibited, if this beginning event happens before the blood clot is partially absorbed. Currently, our group is developing algorithms to quantitatively assess the CBF from OMAG measurements, so that accurate angiodynamics following TBI can be provided.

Acknowledgments

This research was supported in part by grants from the National Institutes of Health (Nos. R01EB009682, R01HL093140, and R01DC010201) and the American Heart Association (0855733G).

References

1. C. Werner and K. Engelhard, "Pathophysiology of traumatic brain injury," *Br. J. Anaesth.* **99**(1), 4–9 (2007).
2. G. J. Bouma and J. P. Muizelaar, "Cerebral blood flow, cerebral blood volume, and cerebrovascular reactivity after severe head injury," *J. Neurotrauma* **9**, S333–S348 (1992).
3. O. Sakurada, C. Kennedy, J. Jehle, J. D. Brown, G. L. Carbin, and L. Sokoloff, "Measurement of local cerebral blood flow with iodo [14C] antipyrine," *Am. J. Physiol.* **234**, H59–66 (1978).
4. A. K. Dunn, H. Bolay, M. A. Moskowitz, and D. A. Boas, "Dynamic imaging of cerebral blood flow using laser speckle," *J. Cereb. Blood Flow Metab.* **21**, 195–201 (2001).
5. F. Calamante, D. L. Thomas, G. S. Pell, J. Wiersma, and R. Turner, "Measuring cerebral blood flow using magnetic resonance imaging techniques," *J. Cereb. Blood Flow Metab.* **19**(7), 701–735 (1999).
6. T. Misgeld and M. Kerschensteiner, "In vivo imaging of the diseased nervous system," *Nat. Rev. Neurosci.* **7**(6), 449–463 (2006).
7. R. K. Wang, S. L. Jacques, Z. Ma, S. Hurst, S. Hanson, and A. Gruber, "Three dimensional optical angiography," *Opt. Express* **15**(7), 4083–4097 (2007).
8. R. K. Wang and S. Hurst, "Mapping of cerebrovascular blood perfusion in mice with skin and cranium intact by optical micro-angiography at 1300 nm wavelength," *Opt. Express* **15**(18), 11402–11412 (2007).
9. C. A. Guyton, "Local and humoral control of blood flow by the tissue," *Textbook of Medical Physiology*, pp. 195–202, W.B. Saunders, Philadelphia, (2006).
10. R. Morgan, C. W. Kreipke, G. Roberts, M. Bagchi, and J. A. Rafols, "Neovascularization following traumatic brain injury: possible evidence for both angiogenesis and vasculogenesis," *Neurol. Res.* **29**(4), 375–381 (2007).